Supporting Information

Highly Efficient and Sustainable Synthesis of Neoglycoproteins using Galactosidases

P. Hoyos,[†] T. Bavaro, [‡*] A. Perona, [†] A. Rumbero, [‖] Sara Tengattini, [‡] M. Terreni, [‡] and María J. Hernáiz[†*]

[†] Chemistry in Pharmaceutical Sciences Department, Faculty of Pharmacy, Complutense University of Madrid, Pz/ Ramón y Cajal s/n. 28040 Madrid, Spain.

[‡] Department of Drug Sciences, University of Pavia, Viale Taramelli 12, I-27100 Pavia, Italy.

[‖] Organic Chemistry Department, Autonoma University of Madrid, Cantoblanco, 28049 Madrid, Spain

[*]E-mail: mjhernai@ucm.es

1. Synthesis of Synthesis of GlcNAcSCH$_2$CN S3

2. Production of enzyme and purification S5

3. Enzyme activity assay S5

4. Computational methods S6

5. ESI-MS spectrum of Galβ(1-6)GlcNAcSCH$_2$CN S9

6. Glycosylation of ribonuclease A with Gal β(1→6)GlcNAc-IME S9

7. Figures Computational methods S11

Figure S1 S11

Figure S2 S11

Figure S3 S11

Figure S4 S12

Figure S5 S12

Figure S6 S13

Figure S7 S13

Figure S8 S14

Figure S9 S14

Figure S10 S15

Figure S11 S15

8. Refereces S16

1. Synthesis of 1-thio-S-cyanomethyl-2-acetamido-2-deoxy-β-D-glucopyranoside ($GlcNAcSCH_2CN$).

Synthesis of 1-thio-S-cyanomethyl-2-acetamido-3,4,6,-tri-*O*-acetyl-2-deoxy-α-D-glucopyranoside was performed according to the procedure previously reported and following the net scheme.[1]

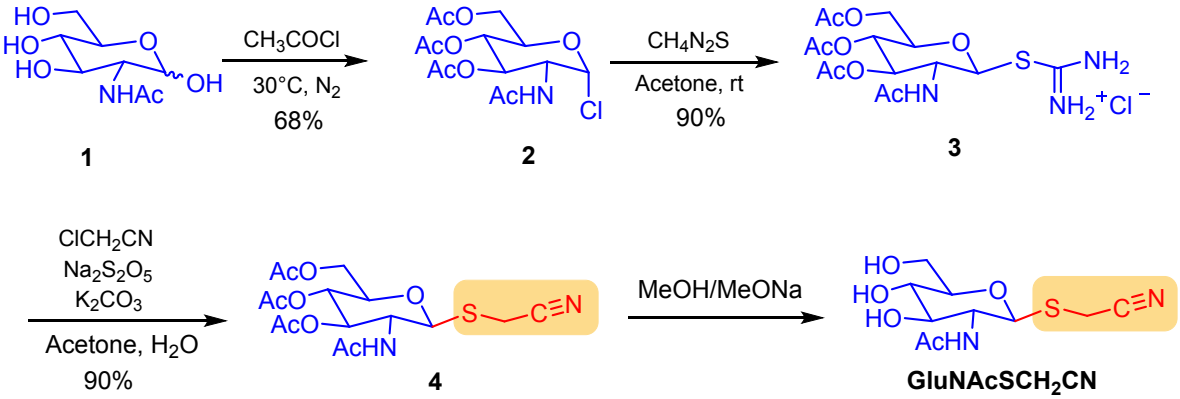

Scheme S1. Synthesis of GlcNAcSCH2CN

1-Chloro-2-acetamido-3,4,6,-tri-*O*-acetyl-2-deoxy-α-D-glucopyranoside (2): *N*-Acetyl glucosamine (**1**, 2 g, 9,041 mmol) was suspended in acetyl chloride (20 mL) in the presence of activated molecular sieves 4 Å, and was stirred for 48 hours at 30°C and the reaction was monitored by TLC (dichloromethane/methanol, 95:5). The solution was diluted with dichloromethane and poured into ice cold water (25 mL). The aqueous phase was extracted 3 times with dichloromethane and the organic layers were combined and washed with saturated sodium bicarbonate, dried over anhydrous Na_2SO_4, filtered and concentrated *in vacuo*. The crude solid was purified by flash chromatography (ethyl acetate/hexane, 7:3) gave a white solid of **2a** with a yield of 68%. R_f = 0,71 (dichloromethane/methanol, 95:5).

1-Thiourea-2-acetamido-3,4,6,-tri-*O*-acetyl-2-deoxy-α-D-glucopyranoside (3): 1-Chloro-2-acetamido-3,4,6,-tri-*O*-acetyl-2-deoxy-α-D-glucopyranoside (**2**, 1 g, 2.734 mmol) and thiourea (0.38 g, 5 mmol) were dissolved in anhydrous acetone (10 ml) under an atmosphere of N_2 in the presence of activated molecular sieves 4 Å. The mixture was refluxed for 3 hours at room temperature. A white precipitate had formed and compound **3a** was isolated by filtration, washed with ethanol and concentrated *in vacuo* gave pure product with a yield of 90%.

1-Thio-*S*-cyanomethyl-2-acetamido-3,4,6-tri-*O*-acetyl-2-deoxy-β-D-glucopyranoside (4): 1-Thiourea-2-acetamido-3,4,6,-tri-*O*-acetyl-2-deoxy-α-D-glucopyranoside (**3**, 0.245 g, 0.554 mmol) was dissolved in 1:1 water:acetone mixture (2.6 mL) and sodium metabisulphite (0.212 g, 1.115 mmol), potassium carbonate (0.093 g, 0.672 mmol) and chloroacetonitrile (0.712 mL, 20 eq) were added. The mixture was stirred at room temperature and reaction was monitored by TLC. Upon completion, 8 mL of ice water were added to the solution that was stirred for 45 minutes. The reaction was extracted with dichloromethane and the combined organics extracts were washed with brine and dried over anhydrous Na_2SO_4 and concentrated *in vacuo*, affording **4** with a yield of 98%. R_f= 0.71 (dichloromethane/methanol, 95:5, v/v).

Synthesis of GlcNAcSCH$_2$CN. 1-thio-*S*-cyanomethyl-2-acetamido-3,4,6-tri-*O*-acetyl-2-deoxy-β-D-glucopyranoside (1 g, 3.62 mmol) was dissolved in 40 mL of dry methanol. 1 wt% of sodium methoxide (0.01 g, 0.19 mmol) was added. The reaction mixture was reacted for 24 h under nitrogen. After, TLC (mobile phase: ethyl acetate) indicated the complete consumption of starting material and the formation of the product (R_f 0.1). The reaction mixture was concentrated *s.v.* and the solid was crystallised from hot methanol to obtain 0.4 g of white solid (56% yield).

2. Production of enzyme and purification

Recombinant β-galactosidase from *Bacillus circulans* ATTC 31382 β-Gal-3-NTag was cloned in *E. coli* BL21 using pET28bþ vectors (Novagen). *E. coli* cultures were grown aerobically at 37 ºC in LB broth with kanamycin (50 mg L-1) and induced with IPTG (isopropyl β-D-thiogalactopyranoside, 1 mM) at 37 ºC for 5 h. Cells were disrupted by sonic disruption, unbroken cells and insoluble debris were eliminated by centrifugation (14.000 g for 15 min at 4 ºC). The solution obtained was passed through a Ni^{2+}-agarose column (5 ml) according to manufacturer's protocol (BioRad). Fractions were monitored by absorbance at 280 nm, and those containing the protein were concentrated and desalted in an Amicon ultra centrifuge filter (Millipore). Protein quantification was done by Bradford method, using bovine serum albumin (BSA) as standard.

3. Enzyme activity assay

Hydrolytic activity was determined spectrophotometrically by quantification of pNP (p-nitrophenol) liberated from the hydrolysis of p-NP- β-D-galactopyranoside 5 mM in buffer (sodium phosphate buffer 50 mM, pH 7 for the recombinant β-galactosidase from *B. circulans* and Tris/HCl buffer 10 mM, pH 7.3 for β -galactosidase from *E. coli*) in a 2 mL cell by measuring the increase in absorbance at 410 nm during 3 min at 37 uC. One enzymatic unit was defined as the amount of protein that hydrolyses 1 μmol of pNP-β-Gal per minute under the conditions described before.

4. Computational methods

Starting structure of the protein. The Cartesian coordinates for a 3D model of the β-Galactosidase from *E. coli* and from *Bacillus circulans* ATTC 3182 were taken directly from the PDB (accession code 1JZ7[2] and 4MAD[3] respectively). All water molecules and ligands were removed. The structures setup entailed adding hydrogen atoms, to assign atom types and charges according to AMBER ff14SB force field[4], and to determine the protonation state of titratable residues at pH 7 using H++ web server, version 3.0.[5,6,7] The Poisson-Boltzmann (PB) method[8] was used, at pH 7 for *E. col*i and pH 6 for *B. circulans*, 0.15 M salt concentration, with internal and external dielectric constants of 4 and 80. In both structures the nucleophilic glutamic[9] acid was glycosylated using the galactopyranose moiety. The resultant glycosylated enzymes were further minimized with the same force field.

Ligand preparation. 3D structure for $GlcNAcSCH_2CN$ was built using glycam carbohydrate builder web server and the interactive molecular graphics program PyMOL[10] which was also employed for structure visualization, molecular editing. The ground state geometry of the ligand was optimized and fitted to the atoms as AMBER atom types and RESP charges using the program antechamber (AmberTools16,[11] URL:ambermd.org).

Docking. The 3D geometry of the complexe formed by the glycosylated enzymes with $GlcNAcSCH_2CN$ was deduced by using AutoDock 4.2.[12] $GlcNAcSCH_2CN$ was docked in a well-defined cavity where the catalytic pair of glutamic acids are located (residues GLU-461 and glycosylated-GLU-537 for *E. Coli* [2] and GLU-157 and glycosylated-GLU-233 for *B. circulans*).[9] The default Lamarckian genetic algorithm parameters and a grid of 50 x 50 x 50 points (spacing 0.3675 Å) were chosen.

The most favourable poses were selected according to its predicted docking energy and the distances between glycosylated glutamic acid and GlcNAcSCH$_2$CN. Two complexes were selected for *B. circulans* enzyme, one with distances that could allow the 1-3 reaction, and one that could allow the 1-6 reaction. For *E. coli* only the complex with distances that allow the 1-6 reaction was selected. The resultant complexes were used as the starting point for molecular dynamics studies.

Molecular dynamics simulation in water. The complexes were immersed in cubic boxes of TIP3P water molecules[13] large enough to guarantee that the shortest distance between the solute and the edge of the box was greater than 15 Å. Counterions were also added to maintain electro neutrality. We performed molecular dynamics simulations using AMBER16 package.[11] The starting structure, prepared as indicated above, was simulated in the NPT ensemble with the periodic boundary conditions and particle mesh Ewald method to treat long-range electrostatic effects.[14] The protocol was as follows: Three consecutive minimizations were performed: (i) involving only hydrogen atoms, (ii) involving only the water molecules and ions, and (iii) involving the entire system. The system was then heated and equilibrated in two steps: (i) 20 ps of MD heating the whole system from 100 to 300 K and (ii) equilibration of the entire system during 100 ps at 300 K. The equilibrated structure was the starting points for 40 ns of MD simulations carried out using the *pmemd_cuda.SPFP* at constant temperature (300K) and pressure (1 atm) and the standard ff14SB force field parameters. The constraint algorithm SHAKE[15] was used to keep bonds involving H atoms at their equilibrium length, allowing a 2 fs time step for the integration of Newton's equations of motion. The *cpptraj* module[16] in AMBER16 was employed for data processing and geometry analysis of the calculated trajectories.

Molecular dynamics simulation in SB2. The complexes were immersed in cubic boxes solvent. The solvent was represented explicitly at the molecular level as a mix of standard TIP3P water molecules and SB2 molecules 2M. As SB2 is not a standard solvent in the AMBER force field, it was necessary to first determine the parameters of the SB2 to perform the simulations. We have use xleap program (AmberTools16,[11] URL:ambermd.org) to draw the molecule and obtain the structure in pdb format. The ground state geometry of SB2 solvent molecule was optimized and fitted to the atoms as AMBER atom types and RESP charges using the program antechamber (AmberTools16,[11] URL:ambermd.org). Parmchk program (AmberTools16,[11] URL:ambermd.org) was used to create force field modification (frcmod) files that fill in missing parameters. To pack the protein inside the mix of solvents box we have used Packmol program.[17,18] Packmol created an initial point for MD simulations of the complexes and the MD simulation protocol described above was carried out.

Analysis of MD trajectories. The stability of the complex was evaluated by calculating the root-mean-square-deviation (RMSD) of the Cα atoms along the trajectories, using their starting structures as reference. The root-mean-square-fluctuation (RMSF) of each residue, relative to the corresponding average value, was calculated once each snapshot had been fitted to its initial structure. The effective binding free energies between the dendrimer and the more relevant residues in the binding site were qualitatively estimated using the program MM-ISMSA. It includes a molecular mechanics (MM) part based on a 12−6 Lennard-Jones potential; an electrostatic component based on an implicit solvent model (ISM) with individual desolvation penalties for each partner in the complex plus a hydrogen bonding term; and a surface area (SA) contribution to account for the loss of water contacts upon complex formation.[19]

5. ESI-MS spectrum of Galβ(1-6)GlcNAcSCH$_2$CN

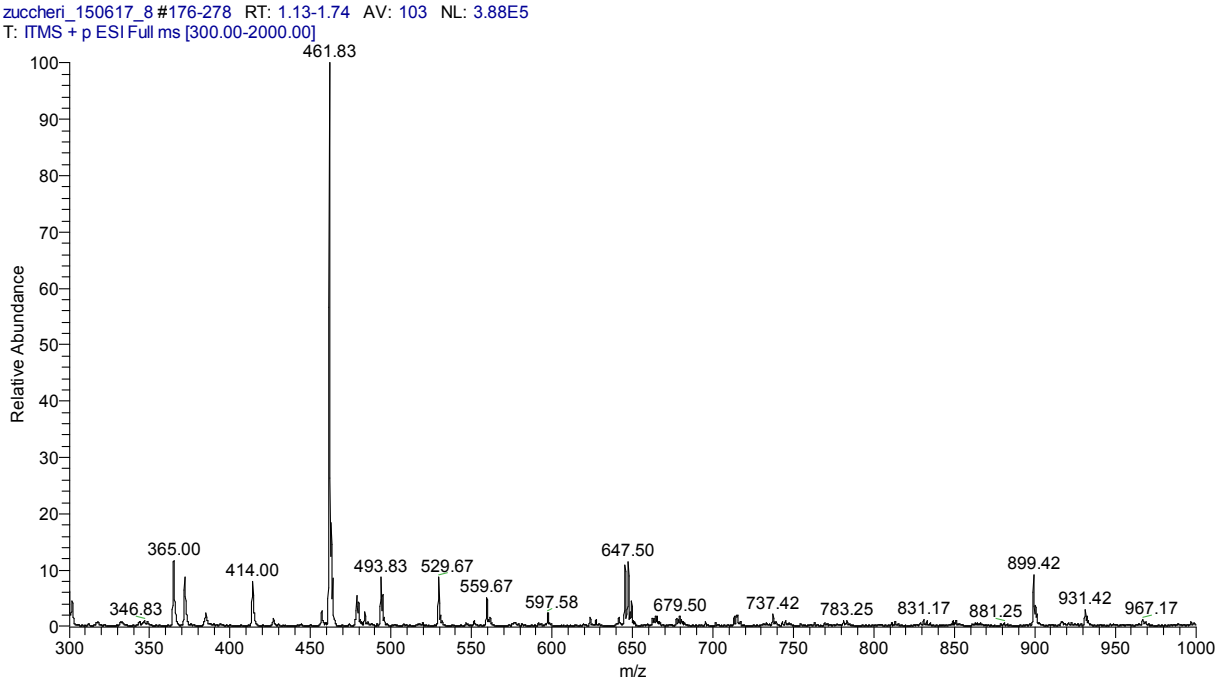

6. Glycosylation of ribonuclease A with Gal β(1→6)GlcNAc-IME

Activation of Gal β(1→6)GlcNAcSCH$_2$CN and synthesis of neo-glycoproteins have been performed according to the method previously reported,[20] with minimal modifications. Briefly, Gal β(1→6)GlcNAcSCH$_2$CN (0.05 g, 0.11 mmol) was dissolved in 5 mL of dry methanol and sodium methoxide (0.009 g, 0.17 mmol) was added. The reaction was reacted for 24h under nitrogen, after which time the reaction mixture was concentrated *in vacuo* and the solid formed was characterized by MS analysis.

MS: m/z = 493.83 [M + Na]+ (calcd 493.49).

The glycosylation reaction was carried out in sodium tetraborate buffer 100 mM, pH 9.5.Ribonuclease A was dissolved in the buffer at a concentration of 1 mg mL−1, then to the solution was added Gal β(1→6)GlcNAc-IME to a final glycoside/protein molar ratio of 100/1. The reaction mixture was vortexed for 1 minute and incubated for 24 hours at 25 °C under continuous stirring.

After 24 h, sample was submitted to seven ultracentrifugation steps of 20 min at 13000 rpm and 4 °C using filter with loading capacity of 500 μL and Nominal Molecular Weight Limit (NMWL) of 3 kDa, and deionized water as washing solvent. Glycosylation yield was determined by direct infusion ESI-MS. Purified neo-glycoprotein was diluted to a final concentration of 0.3 mg mL^{-1} in H_2O:ACN, 50:50 containing 0.05% TFA and introduced into the mass spectrometer with a syringe pump at a flow rate of 10 μL min^{-1}. Full scan intact MS experiments were carried out under the following instrumental conditions: positive ion mode, mass range 700–2000 m/z, source voltage 4.5 kV, capillary voltage 35 V, sheath gas 15, auxiliary gas 2, capillary temperature 220 °C, tube lens voltage 140 V.

The spectra were deconvoluted with Bioworks Browser (Thermo Electron, revision 3.1). The identities of RNase A and its glycoforms were assigned on the basis of the average molecular weight in the deconvoluted spectra and their relative abundance determined by the relative intensities of the relative peaks.

7. Computational methods figures

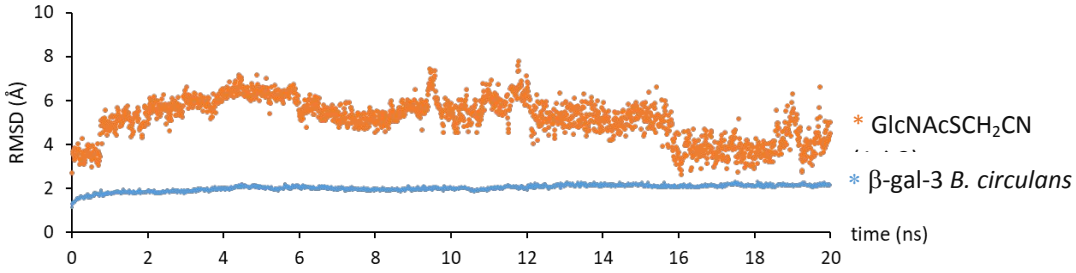

Figure S1. RMSD values relatives to the starting structure along 20 ns of MD simulation in H_2O of *Bacillus circulans* ATCC 31382 β-gal-3 complexed to $GlcNAcSCH_2CN$ with geometrical orientation for **1→3** glycosylation reaction. The Y axis shows the RMSD values in Å and the X axis the time in nanoseconds. RMSD values are represented in blue for the protein β-gal-3 and in orange for the sugar.

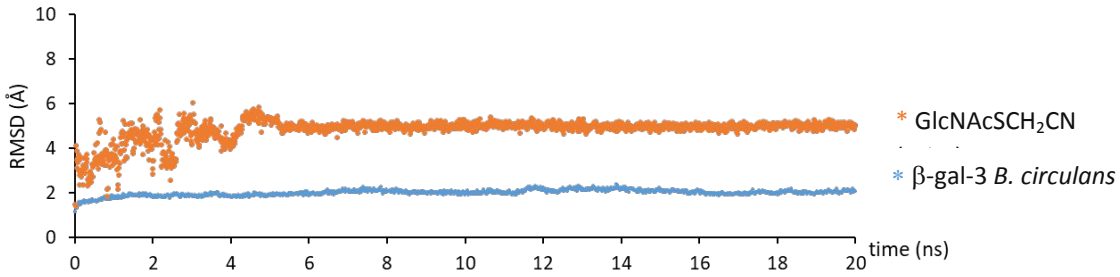

Figure S2. RMSD values relatives to the starting structure along 20 ns of MD simulation in H_2O of *Bacillus circulans* ATCC 31382 β-gal-3 complexed to $GlcNAcSCH_2CN$ with geometrical orientation for **1→4** glycosylation reaction. The Y axis shows the RMSD values in Å and the X axis the time in nanoseconds. RMSD values are represented in blue for the protein β-gal-3 and in orange for the sugar.

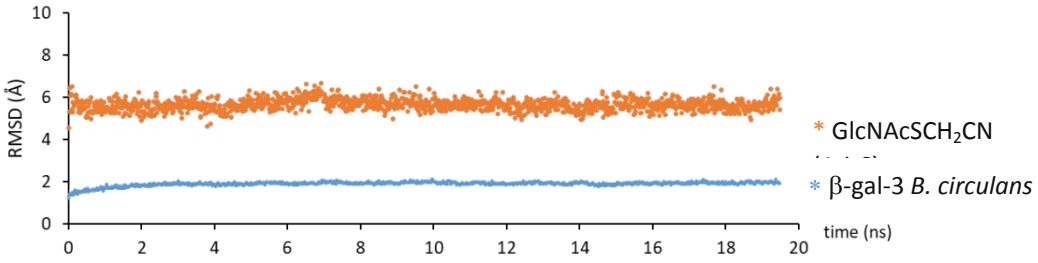

Figure S3. RMSD values relatives to the starting structure along 20 ns of MD simulation in H_2O of *Bacillus circulans* ATCC 31382 β-gal-3 complexed to $GlcNAcSCH_2CN$ with geometrical orientation for **1→6** glycosylation reaction. The Y axis shows the RMSD values in Å and the X axis the time in nanoseconds. RMSD values are represented in blue for the protein β-gal-3 and in orange for the sugar.

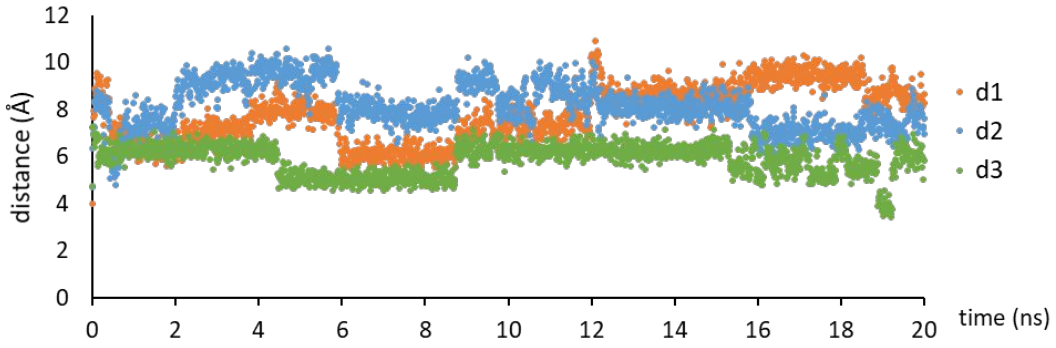

Figure S4. Evolution of d1-d3 (Å) distances along 20 ns of MD simulation in H_2O of *Bacillus circulans* ATCC 31382 β-gal-3 complexed to $GlcNAcSCH_2CN$ with geometrical orientation for **1→3** glycosylation reaction. The Y axis shows the distances values in Å and the X axis the time in nanoseconds, d1 distances are depicted in blue, d2 in orange and d3 in grey.

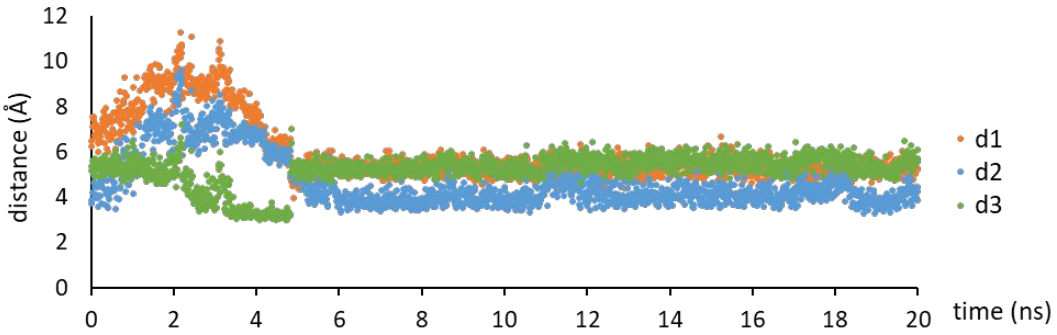

Figure S5. Evolution of d1-d3 (Å) distances along 20 ns of MD simulation in H_2O of *Bacillus circulans* ATCC 31382 β-gal-3 complexed to $GlcNAcSCH_2CN$ with geometrical orientation for **1→4** glycosylation reaction. The Y axis shows the distances values in Å and the X axis the time in nanoseconds, d1 distances are depicted in blue, d2 in orange and d3 in grey.

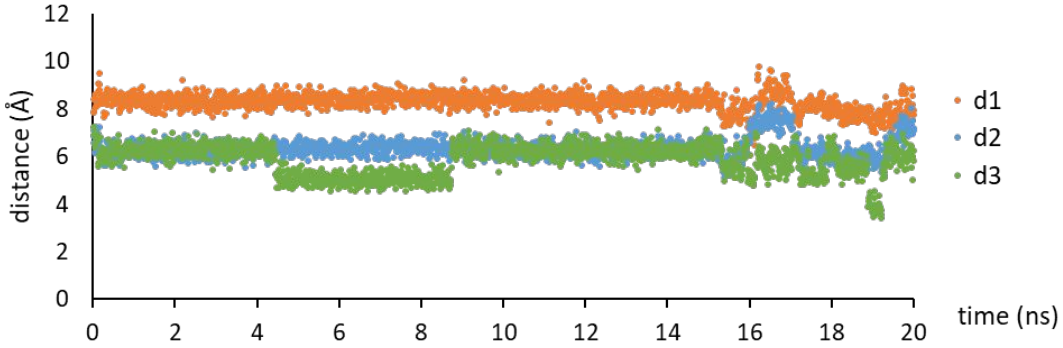

Figure S6. Evolution of d1-d3 (Å) distances along 20 ns of MD simulation in H_2O of *Bacillus circulans* ATCC 31382 β-gal-3 complexed to $GlcNAcSCH_2CN$ with geometrical orientation for **1→6** glycosylation reaction. The Y axis shows the distances values in Å and the X axis the time in nanoseconds, d1 distances are depicted in blue, d2 in orange and d3 in grey.

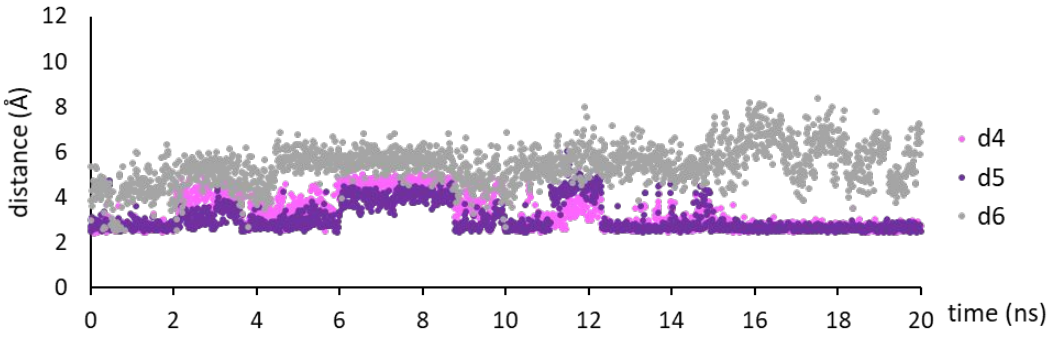

Figure S7. Evolution of d4-d6 (Å) distances along 20 ns of MD simulation in H_2O of *Bacillus circulans* ATCC 31382 β-gal-3 complexed to $GlcNAcSCH_2CN$ with geometrical orientation for **1→3** glycosylation reaction. The Y axis shows the distances values in Å and the X axis the time in nanoseconds, d4 distances are depicted in pink, d5 in purple and d6 in grey.

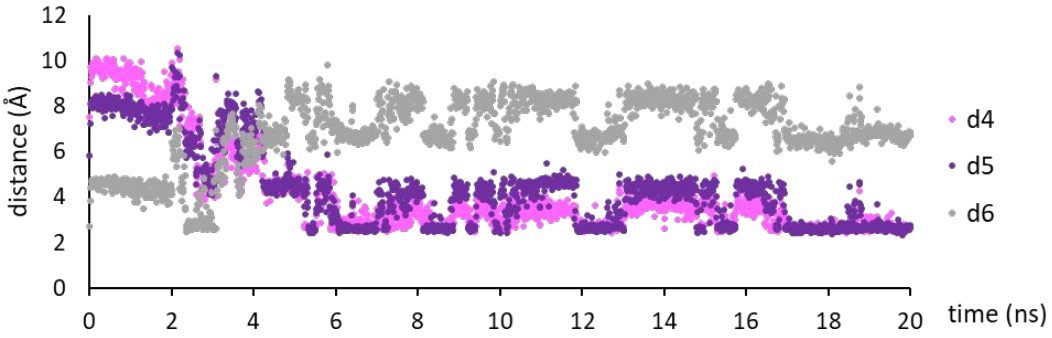

Figure S8. Evolution of d4-d6 (Å) distances along 20 ns of MD simulation of in H_2O *Bacillus circulans* ATCC 31382 β-gal-3 complexed to $GlcNAcSCH_2CN$ with geometrical orientation for **1→4** glycosylation reaction. The Y axis shows the distances values in Å and the X axis the time in nanoseconds, d4 distances are depicted in pink, d5 in purple and d6 in grey.

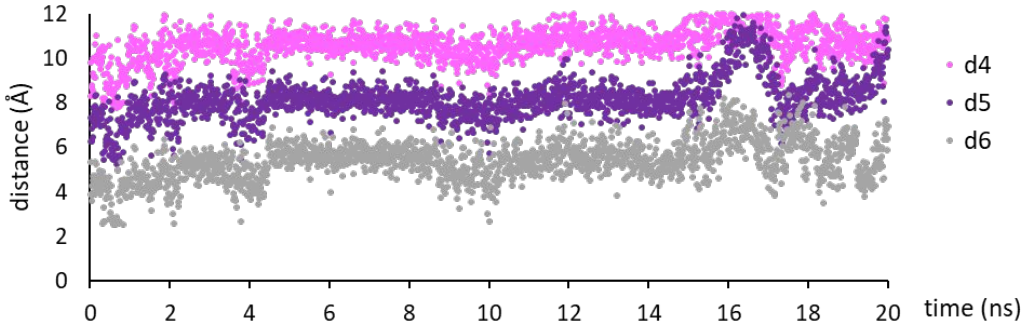

Figure S9. Evolution of d4-d6 (Å) distances along 20 ns of MD simulation in H_2O of *Bacillus circulans* ATCC 31382 β-gal-3 complexed to $GlcNAcSCH_2CN$ with geometrical orientation for **1→6** glycosylation reaction. The Y axis shows the distances values in Å and the X axis the time in nanoseconds, d4 distances are depicted in pink, d5 in purple and d6 in grey.

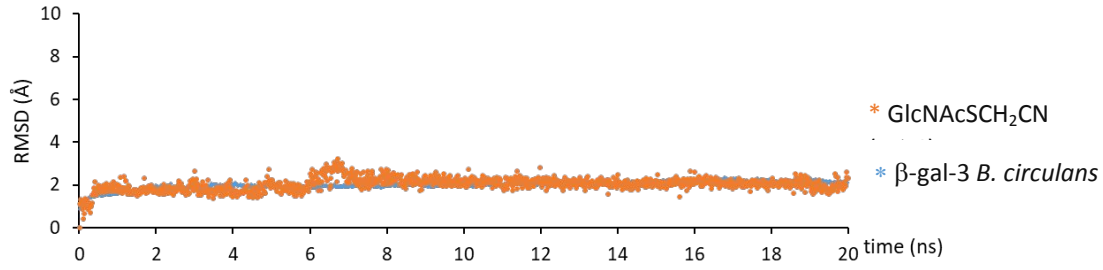

Figure S10. RMSD values relatives to the starting structure along 20 ns of MD simulation in H_2O/SB2 of *Bacillus circulans* ATCC 31382 β-gal-3 complexed to $GlcNAcSCH_2CN$ with geometrical orientation for **1→6** glycosylation reaction. The Y axis shows the RMSD values in Å and the X axis the time in nanoseconds. RMSD values are represented in blue for the protein β-gal-3 and in orange for the sugar.

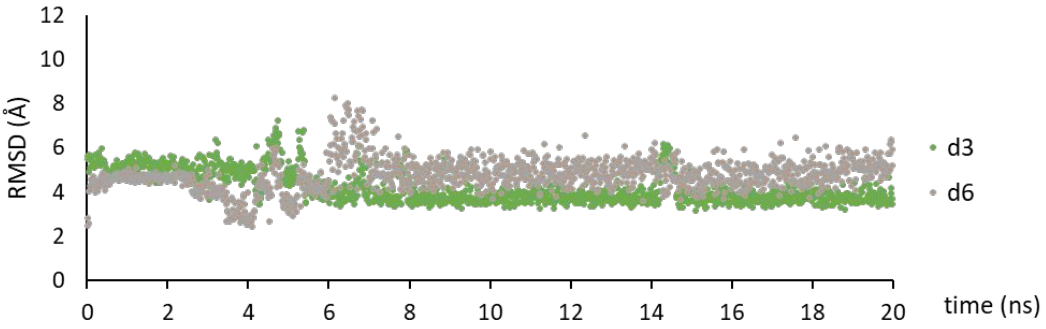

Figure S11. Evolution of d3 and d6 (Å) distances along 20 ns of MD simulation in H_2O/SB2 of *Bacillus circulans* ATCC 31382 β-gal-3 complexed to $GlcNAcSCH_2CN$ with geometrical orientation for **1→6** glycosylation reaction. The Y axis shows the distances values in Å and the X axis the time in nanoseconds, d3 distances are depicted in green and d6 in grey.

8. References

1. Temporini, C.; Bavaro, T.; Tengattini, S.; Serra, I.; Marrubini, G.; Calleri, E.; Fasanella, F.; Piubelli, L.; Marinelli, F.; Pollegioni, L.; Speranza, G.; Massolini, G.; Terreni, M., Liquid Chromatography–Mass Spectrometry Structural Characterization of Neoglycoproteins Aiding the Rational Design and Synthesis of a Novel Glycovaccine for Protection against Tuberculosis. *J. Chromatogr. A* **2014,** *1367*, 57-67. DOI: 10.1016/j.chroma.2014.09.041
2. Juers, D. H.; Heightman, T. D.; Vasella, A.; McCarter, J. D.; Mackenzie, L.; Withers, S. G.; Matthews, B. W., A structural View of the Action of *Escherichia coli* (lacZ) β-galactosidase. *Biochemistry* **2001,** *40* (49), 14781-94. DOI: 10.1021/bi011727i
3. Henze, M.; You, D. J.; Kamerke, C.; Hoffmann, N.; Angkawidjaja, C.; Ernst, S.; Pietruszka, J.; Kanaya, S.; Elling, L., Rational Design of a Glycosynthase by the Crystal Structure of β-galactosidase from *Bacillus circulans* (BgaC) and its use for the Synthesis of *N*-acetyllactosamine type 1 Glycan Structures. *J. Biotechnol.* **2014,** *191*, 78-85. DOI: 10.1016/j.jbiotec.2014.07.003
4. Maier, J. A.; Martinez, C.; Kasavajhala, K.; Wickstrom, L.; Hauser, K. E.; Simmerling, C., ff14SB: Improving the Accuracy of Protein Side Chain and Backbone Parameters from ff99SB. *J. Chem. Theory Comput.* **2015,** *11* (8), 3696-3713. DOI: 10.1021/acs.jctc.5b00255.
5. Anandakrishnan, R.; Aguilar, B.; Onufriev, A. V., H++ 3.0: Automating p K Prediction and the Preparation of Biomolecular Structures for Atomistic Molecular Modeling and Simulations. *Nucleic Acids Res.* **2012,** *40* (W1), W537-W541. DOI: 10.1093/nar/gks375
6. Myers, J.; Grothaus, G.; Narayanan, S.; Onufriev, A. A Simple Clustering Algorithm can be Accurate Enough for use in Calculations of pKs in Macromolecules. *Proteins,* **2006,** *63* (4), 928-938. DOI: 10.1002/prot.20922
7. Gordon, J. C.; Myers, J. B.; Folta, T.; Shoja, V.; Heath, L. S.; Onufriev, A., H++: a Server for Estimating p K as and Adding Missing Hydrogens to Macromolecules. *Nucleic Acids Res.* **2005,** *33* (suppl_2), W368-W371. DOI: 10.1093/nar/gki464
8. Honig, B.; Nicholls, A., Classical Electrostatics in Biology and Chemistry. *Science* **1995,** *268* (5214), 1144-1149. DOI: 10.1126/science.7761829
9. Bayón, C.; Cortés, Á.; Aires, A.; Civera, M. C.; Hernáiz, M. J., Highly Efficient and Regioselective Enzymatic Synthesis of β-(1→3) Galactosides in Biosolvents. *RSC Adv.* **2013,** *3 (30)* 12155-12163. DOI: 10.1039/c3ra40860d
10. Schrödinger, L., The PyMOL Molecular Graphics System, . DeLano, W. L., Ed. 2013.
11. Case, D.; JTB, R.; Betz, D.; Cerutti III, T.; Cheatham III, T.; Darden, R., Duke, TJ Giese, H. Gohlke, AW Goetz, N. Homeyer, S. Izadi, P. Janowski, J. Kaus, A. Kovalenko, TS Lee, S. LeGrand, P. Li, T. Luchko, R. Luo, B. Madej, KM Merz, G. Monard, P. Needham, H. Nguyen, HT Nguyen, I. Omelyan, A. Onufriev, DR Roe, A. Roitberg, R. Salomon-Ferrer, CL Simmerling, W. Smith, J. Swails, R.C. Walker, J. Wang, R.M. Wolf, X. Wu, D.M. York and P.A. Kollman Amber **2015**.
12. Morris, G. M.; Huey, R.; Lindstrom, W.; Sanner, M. F.; Belew, R. K.; Goodsell, D. S.; Olson, A. J., AutoDock4 and AutoDockTools4: Automated Docking with Selective Receptor Flexibility. *J. Comput. Chem.* **2009,** *30* (16), 2785-2791. DOI: 10.1002/jcc.21256.

13. Jorgensen, W. L.; Chandrasekhar, J.; Madura, J. D.; Impey, R. W.; Klein, M. L., Comparison of Simple Potential Functions for Simulating Liquid Water. *J. Chem. Phys.* **1983,** *79* (2), 926-935. DOI: 10.1063/1.445869
14. Darden, T.; York, D.; Pedersen, L., Particle mesh Ewald: An N· log (N) method for Ewald sums in large systems. *J. Chem. Phys.* **1993,** *98* (12), 10089-10092. DOI: 10.1063/1.464397
15. Ryckaert, J.-P.; Ciccotti, G.; Berendsen, H. J., Numerical Integration of the Cartesian Equations of Motion of a System with Constraints: Molecular Dynamics of n-Alkanes. *J. Comput. Phys.* **1977,** *23* (3), 327-341. DOI: 10.1016/0021-9991(77)90098-5
16. Roe, D. R.; Cheatham III, T. E., PTRAJ and CPPTRAJ: Software for Processing and Analysis of Molecular Dynamics Trajectory Data. *J. Chem. Theory Comput.* **2013,** *9* (7), 3084-3095. DOI: 10.1021 / ct400341p
17. Martinez, J. M.; Martinez, L., Packing Optimization for Automated Generation of Complex System's Initial Configurations for Molecular Dynamics and Docking. *J. Comput. Chem.* **2003,** *24* (7), 819-825. DOI: 10.1002/jcc.10216
18. Martinez, L.; Andrade, R.; Birgin, E. G.; Martinez, J. M., PACKMOL: A Package for Building Initial Configurations for Molecular Dynamics Simulations. *J. Comput. Chem.* **2009,** *30* (13), 2157-2164. DOI: 10.1002/jcc.21224
19. Klett, J.; Núñez-Salgado, A.; Dos Santos, H. G.; Cortés-Cabrera, A. l.; Perona, A.; Gil-Redondo, R. N.; Abia, D.; Gago, F.; Morreale, A., MM-ISMSA: An Ultrafast and Accurate Scoring Function for Protein–Protein Docking. *J. Chem. Theory Comput.* **2012,** *8* (9), 3395-3408.
20. Bavaro, T.; Filice, M.; Temporini, C.; Tengattini, S.; Serra, I.; Morelli, C. F.; Massolini, G.; Terreni, M., Chemoenzymatic Synthesis of Neoglycoproteins Driven by the Assessment of Protein Surface Reactivity. *RSC Adv.* **2014,** *4* (99), 56455-56465.